Pergamon

0967-0645(95)00105-0

Deep-Sea Research II, Vol. 43, No. 2-3, pp. 385-402, 1996
Copyright © 1996 Elsevier Science Ltd
Printed in Great Britain. All rights reserved
0967-0645/96 $15.00 + 0.00

Nitrite distributions and dynamics at Station ALOHA

JOHN E. DORE* and DAVID M. KARL*

(*Received* 5 *September* 1994; *in revised form* 12 *April* 1995; *accepted* 24 *November* 1995)

Abstract—We used a chemiluminescence method to measure nitrite concentrations in the water column at the U.S. JGOFS/WOCE time-series station, ALOHA (22°45′ N, 158° W), from September 1989 to November 1993. We present a detailed time-series of nitrite in the upper 200 m in order to examine the dynamics of the primary nitrite maximum. Our results reveal a double-peaked structure to this feature that is consistent with a vertical separation of the reductive and oxidative microbial processes responsible for nitrite production. The possibility of using the nitrite content of this upper layer as an indicator of nitrogen export from the euphotic zone is explored and rejected.

Midwater nitrite profiles (200–1000 m) show a supra-exponential decrease in concentration with depth and reveal month-to-month variability. Nitrite concentrations in deep waters (1000–4800 m) are in the nanomolar–subnanomolar range, and are similar to Atlantic data, arguing against significant basin-scale differences in the deep nitrite pool. Deep profiles also show measurable variability on both monthly and annual timescales. We speculate that this deep variability may be associated with nitrate reduction by sinking phytoplankton cells. Copyright © 1996 Elsevier Science Ltd

INTRODUCTION

Nitrite, because of its intermediate redox position between ammonium and nitrate, is a useful indicator of the equilibrium state of the oxidative and reductive pathways of the marine nitrogen cycle. Accumulations of nitrite in certain marine strata mark the locations where biologically mediated changes in combined nitrogen occur (Rakestraw, 1936; Vaccaro and Ryther, 1960). Marine biological processes known to produce nitrite include: (i) incomplete assimilatory reduction of nitrate by phytoplankton (Vaccaro and Ryther, 1960; Kiefer *et al.*, 1976) and bacteria (Wada and Hattori, 1972); (ii) chemoautotrophic oxidation of ammonium by nitrifying bacteria (Brandhorst, 1959; Olson, 1981a); and (iii) dissimilatory reduction of nitrate by denitrifying bacteria (Brandhorst, 1959; Fiadeiro and Strickland, 1968; Codispoti and Richards, 1976). In well-oxygenated oceanic waters the latter process is not thought to be significant in nitrite production, however, its relative contribution may increase in the midwater oxygen minimum layer and within the interiors of large particles (Karl *et al.*, 1984).

Despite the long-recognized importance of nitrite as a nitrogen cycle intermediate, methodological constraints have prevented the acquisition of detailed water column nitrite profiles. The standard colorimetric assay (Strickland and Parsons, 1972) is inaccurate at concentrations below about 50 nM, while nitrite levels in the open ocean typically exceed this value only within a narrow layer near the base of the euphotic zone (the primary nitrite

*Department of Oceanography, School of Ocean and Earth Science and Technology, University of Hawaii, Honolulu, HI 96822, U.S.A.

maximum or PNM). Wada and Hattori (1971) developed a sample pre-concentration method capable of extending measurements down to nanomolar levels, but the large sample volumes (500–1000 ml) and multiple manipulations required by their method are undesirable. Routine measurements of the nanomolar and often sub-nanomolar concentrations of nitrite in oceanic surface and sub-PNM waters have only recently become possible with the advent of the chemiluminescent technique, developed by Cox (1980) and modified for seawater samples by Garside (1982). The chemiluminescent method offers excellent precision and accuracy, as well as a low detection limit. This technique has been used successfully to measure low-level nitrite in the Sargasso Sea (Brzezinski, 1988; Zafiriou *et al.*, 1992) and in the north-west Atlantic and the Caribbean Sea (Zafiriou *et al.*, 1992).

The PNM found in oxic oligotrophic seawaters has been traditionally described as a narrow, symmetric peak located near the base of the euphotic layer, with undetectable nitrite concentrations above and below. More recently, the PNM was discovered to be asymmetric, with a pronounced upper peak that slowly decays with depth as a "tail" into deep water (Zafiriou *et al.*, 1992). This asymmetric structure is consistent with that predicted from the PNM model of Kiefer and Kremer (1981), which assumed that the source of nitrite was nitrate reduction by phytoplankton. However, variations of the upper PNM structure also have been described, including enigmatic double maxima and smooth vertically-mixed profiles (Wada and Hattori, 1991). Also, ^{15}N tracer experiments have documented production of nitrite within the PNM via both nitrification and nitrate reduction, with the former usually exceeding the latter in rate (Miyazaki *et al.*, 1973, 1975; Olson, 1981b; Ward *et al.*, 1989). Still, few data exist for the oligotrophic waters of the North Pacific gyre (Olson, 1981b). Through repeated measurements covering both daily and yearly time scales at a single location, we hoped to elucidate the "normal" structure of the PNM and the types of variability that could be expected, and to look for clues as to the processes responsible for nitrite production.

We report here on the water-column nitrite distributions measured at the US-JGOFS/WOCE time-series station, ALOHA, in the North Pacific subtropical gyre over the period September 1989–November 1993. Though some deep profiles (to between 1000 m and the seafloor at about 4800 m) are presented, most of the data are from the upper 200 m, where we have extensively examined the structure and variability of the PNM. For correlative purposes, we include some data on [nitrite + nitrate] distributions as well. We are aware of only one other low-level nitrite data set from the North Pacific (Wada and Hattori, 1972), and believe the present nitrite data represent both the first from this region utilizing the chemiluminescent technique and the first multiyear time-series study of nitrite in the Pacific.

MATERIALS AND METHODS

Station location

All sampling was performed during the regular monthly cruises of the Hawaii Ocean Time-series (HOT) project to the deep-water station, ALOHA (A Long-term Oligotrophic Habitat Assessment; Karl and Lukas, 1996). Station ALOHA is defined as a six nautical-mile radius circle centered at 22°45′ N, 158° W, about 100 km north of Kahuku Pt, Oahu, Hawaii (Fig. 1); every effort is made to sample only within this circle. The site was chosen to be representative of the oligotrophic gyre of the North Pacific Ocean. Between September

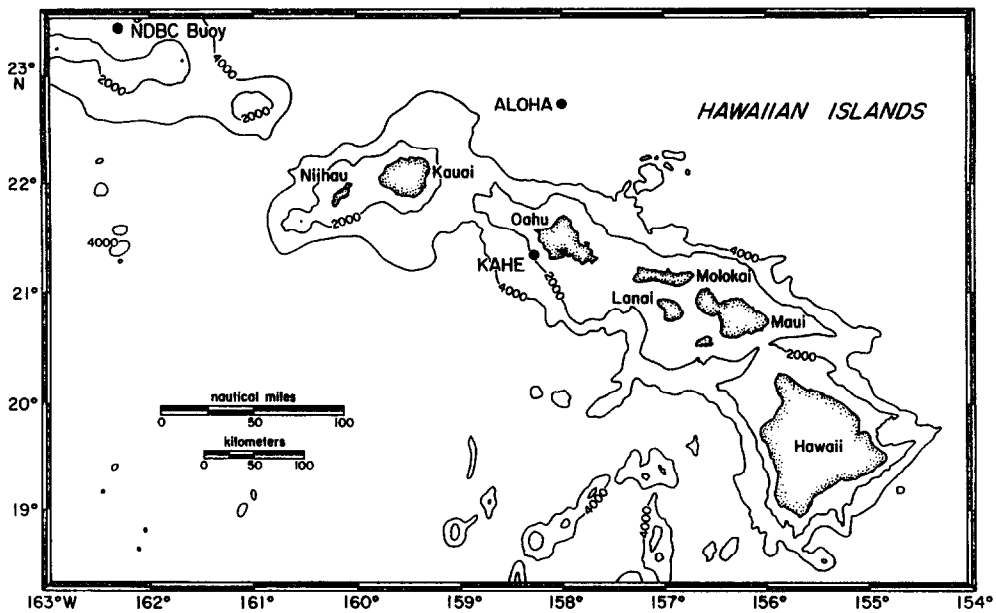


Fig. 1. Location of Sta. ALOHA north of the island of Oahu, Hawaii. The 2000 m and 4000 m isobaths are displayed as solid contour lines. Also shown are nearshore Sta. Kahe and a weather buoy operated by the National Data Buoy Center from which sea surface temperature, wind speed and direction, wave height and wave spectrum data were obtained.

1989 and November 1993 the HOT project completed 41 cruises to Station ALOHA. We obtained at least one upper water column (0–200 m) profile of nitrite from 31 of these cruises, and multiple profiles from eight of them. Midwater profiles (200–1000 m) and deep profiles (1000–4800 m) were obtained from seven cruises. Cruise dates and vessels are listed elsewhere (Karl and Lukas, 1996).

Sampling

Sample collection was performed using a 24-place rosette with 12-l PVC bottles, equipped with a SeaBird CTD, a Beckman polarographic oxygen sensor and a SeaTech flash fluorometer. Light levels and attenuation were determined using a Licor on-deck cosine collector and a Biospherical underwater profiling natural fluorometer. CTD protocols followed WOCE standards described in Bingham and Lukas (1996).

Individual water samples were drawn using clean Tygon tubing into 125-ml acid-washed polyethylene bottles. For each rosette position sampled, the tubing was thoroughly flushed, and each sample bottle was rinsed three times with sample before filling. Particulate matter for chlorophyll-*a* determinations was concentrated by filtration and extracted in acetone for later analysis by fluorometry as described in Letelier *et al.* (1996). Nitrite and other nutrient samples were immediately placed in a −20°C freezer without filtration and kept frozen until the day of analysis. Details of our standard nutrient analyses are given in Dore *et al.* (in press). A free-floating sediment trap array was used for the collection of sinking particulate matter. Details of our sediment trap protocols and particulate analyses are presented in Karl *et al.* (1996).

Chemiluminescent analyses

Frozen samples were thawed slowly in a bath of room-temperature water a few hours before analysis. Subsamples (10 ml) were introduced into the reaction apparatus using a clean syringe. Nitrite concentration ($[NO_2^-]$) was determined through wet chemical reduction using sodium iodide and glacial acetic acid, and subsequent detection of the nitric oxide (NO) produced with an Antek model 720 chemiluminescent nitrogen analyzer. Similarly, nitrite + nitrate concentration ($[NO_2^- + NO_3^-]$) was determined after reduction to NO using ferrous ammonium sulfate, ammonium molybdate and concentrated sulfuric acid. Reagents were pre-sparged with the Ar carrier gas and so introduced no blank. Both procedures followed the methods described by Garside (1982) with no major modifications. Occasionally, chemiluminescent $[NO_2^- + NO_3^-]$ analyses were not performed; in these cases standard automated colorimetric analyses were used instead (Dore *et al.*, in press). All nitrite data presented here were determined by chemiluminescence.

Detection limits, precision and accuracy

Standards were prepared fresh by volumetric serial dilutions of a primary 10 mM stock ($NaNO_2$ or KNO_3) with distilled deionized water (DDW). Accuracy was maintained by including dilutions of CSK certified reference standards (Ambe, 1978) in each analytical run; these always agreed with our standards to within about $\pm 2\%$.

For $[NO_2^-]$ analyses, the lowest concentration of standard to give a reliably readable signal was 0.2 nM. At the same time, our DDW diluent, many samples from the surface mixed layer, and some from deep waters produced zero counts on the detector (i.e. the system blank was zero and indistinguishable from some samples). From this we estimate the absolute detection limit to be approximately 0.1–0.2 nM. Quantification of samples below 1 nM is questionable, though, because the precision (standard deviation of duplicate or triplicate analyses of individual standards or samples) at concentrations < 50 nM averaged ± 0.5 nM. We therefore cannot compare directly individual samples below 1 nM, but we can with some confidence compare multi-point trends at these low levels. At concentrations above 50 nM, the average precision was $\pm 1.6\%$.

For $[NO_2^- + NO_3^-]$ analyses, the lowest standard used was 1.0 nM. Although for these analyses DDW consistently gave a signal (i.e. the system blank was non-zero), the signal from the 1 nM standard was always significantly higher. Average precision was similar to that for nitrite alone, but low-end variability leads us to estimate our detection limit at about 1–2 nM.

Precautions

Because the concentrations of nitrite in these waters are often at or near detection limits, care must be taken to avoid contamination. On board a research vessel, stack gases containing NO and nitrogen dioxide (NO_2) can cause interference (Zafiriou *et al.*, 1992). We were careful to minimize possible exposure of the samples to ambient air on deck, and fortunately did not encounter noticeable contamination problems. Natural NO levels in oxic sea waters are too low to interfere with the analyses of nitrite and nitrate (Ward and Zafiriou, 1988).

To avoid wear and tear on the chemiluminescent analyzer and the associated reaction apparatus and to ensure the high quality of the data, we performed analyses at our land-

based laboratory, requiring the preservation and storage of samples. We therefore conducted experiments comparing methods of preservation and shipboard analyses of fresh samples vs later laboratory analyses of stored samples. In the first of these experiments, a 20-l polyethylene carboy was filled with water from just below the PNM (130 m) and returned to our laboratory. Six sets of four replicate 125-ml polyethylene bottles were filled from this carboy; one set was analyzed immediately, while the others were subjected to different treatments before analysis. The treatments included freezing at −20°C (slow), freezing at −70°C (quick), acidification with HCl to a pH of 2.5, and combinations thereof. All unfrozen samples were analyzed within 6 h of the sample splitting. All frozen samples were analyzed after being stored 19 days at −20°C and thawed in a room temperature water bath.

In the second experiment, 34 depths from near-bottom to near-surface were sampled over the course of two casts. From each rosette bottle two or four samples were drawn; half of these were immediately placed in the −20°C freezer. The others were maintained at 4°C and withdrawn a few at a time about 1 h before analysis; all of these at-sea analyses were performed within about 10 h of collection. The frozen samples were returned to land and analyzed 1 week later.

RESULTS AND DISCUSSION

Storage experiments

The results of our first storage experiment confirmed the observation of Takenaka *et al.* (1992) that at low pH, the freezing of an aqueous sample dramatically reduces its nitrite concentration; however, we found no significant differences (at $\alpha = 0.05$) in nitrite concentration between fresh and slow frozen samples at normal seawater pH (Table 1). Quick freezing at −70°C is not recommended, as we found a slight but significant reduction in nitrite concentration when samples were preserved in this manner (Table 1). Takenaka *et al.* (1992) reported that the rate of oxidation of nitrite to nitrate in acidic solutions is accelerated by an increased rate of freezing; it is likely that our observed nitrite loss upon quick freezing is a result of the same process, but is less pronounced due to the higher pH of the seawater medium. We conclude that there is no discernable effect of the freezing process itself when performed at −20°C on a natural seawater sample stored in polyethylene.

Table 1. *Results of an experiment to determine the effects of several sample storage methods on the concentration of nitrite. See text for details of experiment*

Treatment	Nitrite Concentration* (nM)
Fresh	30.2 (±1.0)
Slow frozen (−20°C)	29.5 (±0.6)
Quick frozen (−70°C)	28.6 (±0.8)
Acidified (pH = 2.5)	26.2 (±0.6)
Acidified and slow frozen	0.7 (±0.4)
Acidified and quick frozen	1.1 (±0.4)

*Mean (±1 standard deviation), $n = 4$.

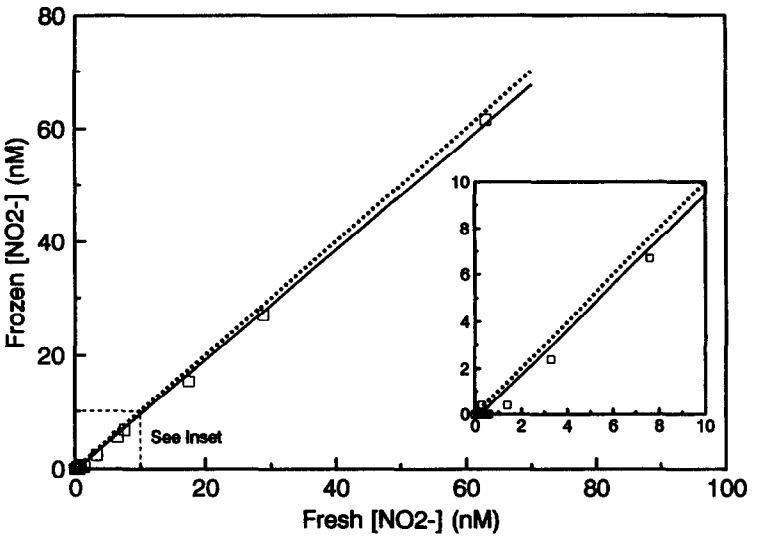


Fig. 2. Results of an experiment to determine the effects of frozen storage of nitrite samples with respect to samples analyzed at sea. The horizontal axis gives the concentration of nitrite in nM as measured at sea; the vertical axis represents the measured concentration of replicate samples frozen and returned to the laboratory for analysis, also in nM. The inset plot is an expansion of the main plot emphasizing those samples with concentrations less than 10 nM. The dotted line is the theoretical 1:1 relation in the absence of treatment effect ($y = x$). The solid line is a reduced major axis model II linear regression of the 34 data points ($y = -0.23 + 0.97x$, $r^2 = 0.999$).

In our second storage experiment, we compared shipboard analysis with laboratory analysis of samples stored frozen, and found the agreement to be excellent (Fig. 2). The largest difference between fresh and frozen samples was 2.1 nM. All samples with fresh values below 10 nM gave frozen values that differed by 1.0 nM or less; those below 1 nM differed by at most 0.6 nM. A model II reduced major axis linear regression of the frozen data onto the fresh data indicates that there was a slight tendency for the fresh values to exceed the frozen values. Furthermore, the three samples exhibiting differences > 1.0 nM were from within the PNM. Biological activity can rapidly alter nitrite concentration in unpreserved samples (Wada and Hattori, 1972; Zafiriou *et al.*, 1992). Considering this observation and our failure to observe a significant "freezing effect" in the first experiment, we suspect that at least part of the slight discrepancy between fresh and frozen analyses is due to increases in nitrite in the fresh samples while they are stored under refrigeration awaiting analysis. Given the above, and the difficulties involved in at-sea analyses, we believe that the analysis of nitrite in seawater is best performed on samples immediately frozen at -20°C and returned to a land-based laboratory.

Nitrite in the upper water column

The upper 200 m of the water column include the nitrite-impoverished surface layer, the "classical" PNM, and the upper reaches of the nitrite tail. An example of what we consider to be a "typical" upper water column nitrite profile under calm conditions is shown in Fig. 3. This profile, taken during HOT-41 (October 1992), shows the major structural features of the PNM that we will focus on throughout this paper. First, we see a nitrite-poor surface

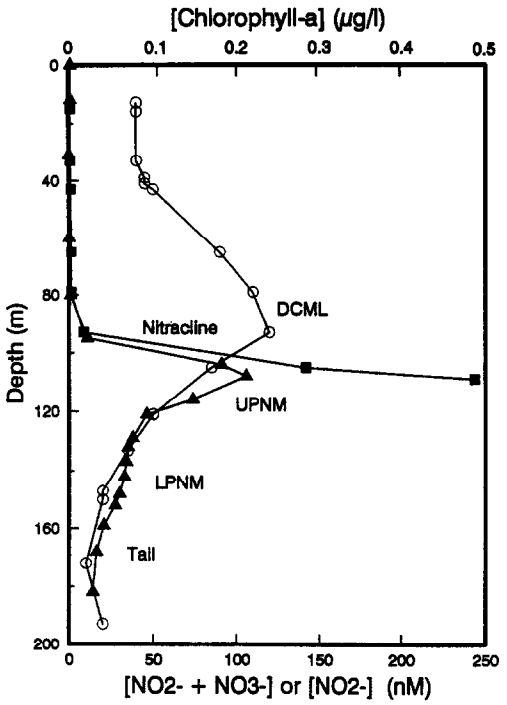


Fig. 3. Upper water column profiles of [nitrite], [nitrite + nitrate] and [chlorophyll-*a*] taken during HOT-41 (October 1992). The bottom horizontal axis shows [nitrite] or [nitrite + nitrate] in nM, the upper horizontal axis shows [chlorophyll-*a*] in $\mu g\ l^{-1}$ and the vertical axis gives the density-averaged depth in m (see text). Solid squares are [nitrite + nitrate], solid triangles are [nitrite] and open circles are [chlorophyll-*a*]. Major features associated with the primary nitrite maximum are labeled and discussed in the text.

layer, with concentrations <2 nM and often at or below the 0.1–0.2 nM detection limit. Second, there is an abrupt increase to an upper primary nitrite maximum (UPNM), where concentrations reach 60–200 nM; this is the "classical" PNM made evident by colorimetric techniques, and is invariably closely associated with the top of the $[NO_2^- + NO_3^-]$ gradient or "nitracline" (Herbland and Voituriez, 1979). The nitracline itself is located within the deep chlorophyll maximum layer (DCML). Third, we find the depth-decaying nitrite tail described by Zafiriou *et al.* (1992), with concentrations of around 50 nM at the base of the UPNM dropping to about 10–25 nM at 200 m. Lastly we see a second nitrite peak below the UPNM, in this case between about 135 and 155 m. This lower primary nitrite maximum (LPNM) varies greatly in magnitude. In the present case it is only barely discernable, but it is often more pronounced, at times rivaling the UPNM in magnitude (Fig. 4). We have found a clearly defined LPNM in approximately one third of the cruises we have examined, and it arguably exists in others; we believe that the double-peaked PNM is not an anomaly, but that the maintenance of two distinct maxima is an indication of a vertical separation of nitrogen-cycle processes in this portion of the water column.

Temporal variability in the upper water column nitrite structure on short timescales (hours to days) can be quite dramatic (e.g. see French *et al.*, 1983). We will assume that within the circle defining Station ALOHA horizontal variability of upper water column nitrite during any given 3-day period is small. While we cannot entirely dismiss the presence

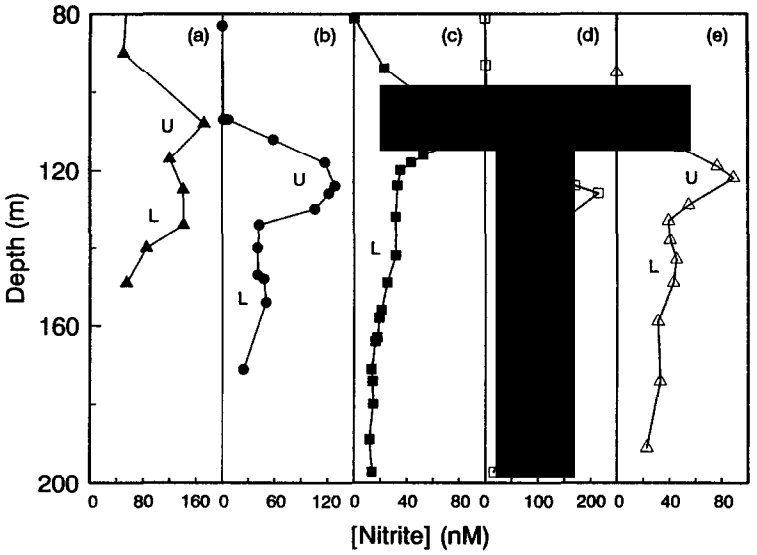


Fig. 4. Individual 80–200 m depth profiles of nitrite displaying two-peaked structure from five HOT cruises. U indicates position of UPNM in each profile, L indicates position of LPNM. $[NO_2^-]$ is reported in nM, density-averaged depth (see text) is given in m. Profiles displayed are from the following cruises: (a) HOT-14, February 1990; (b) HOT-19, July 1990; (c) HOT-22, December 1990; (d) HOT-31, October 1991; (e) HOT-40, September 1992.

of spatial heterogeneity, a published 0–200 m nitrite section (using colorimetric techniques) along 28° N shows little variability between 162°30′ W and 180° W, supporting our assumption (Shulenberger, 1978). Similarly, the section along 155° W presented by Wada and Hattori (1972) shows a strong degree of homogeneity in the vertical distribution of upper water column nitrite between about 15° N and 35° N. Nevertheless, minor spatial differences capable of complicating our temporal study could be masked by the 50 nM contour intervals used by the above authors, and so cannot be completely ruled out. Also, horizontal water mass intrusions bearing different nitrite signatures could potentially complicate the interpretation of temporal changes in nitrite profiles. However, since we are looking here at <3 day timescales, the origin of such intrusions must be local (~ 100 km distant or less), and we have no evidence for horizontal nutrient gradients within 75 km of Station ALOHA. We therefore will assume here that horizontal variability and horizontal water mass motions are not significantly affecting nitrite distributions in the upper 200 m.

Given our assumption of relative spatial homogeneity, then, apparent changes in the vertical nitrite structure observed while on station must be the combined result of two phenomena: changes in the positions of features due to vertical physical motions or mixing of the water column, and changes of concentration within features due to biological and chemical transformations of nitrogen species. An example from HOT-19 (July 1990) illustrates both types of alterations (Fig. 5). Two nitrite profiles from casts sampled about 12 h apart are plotted as $[NO_2^-]$ vs depth (for clarity, only the 60–180 m range is shown). The offset between the upper slope of the UPNM in the two casts (Fig. 5(a)) is due to the vertical displacement of isopycnals by an internal wave. In order to filter such short-term vertical motions of the PNM, we employ a density-averaging technique, in which a sampled isopycnal is related to its average depth during the 3 days on station (Fig. 5(b)). When

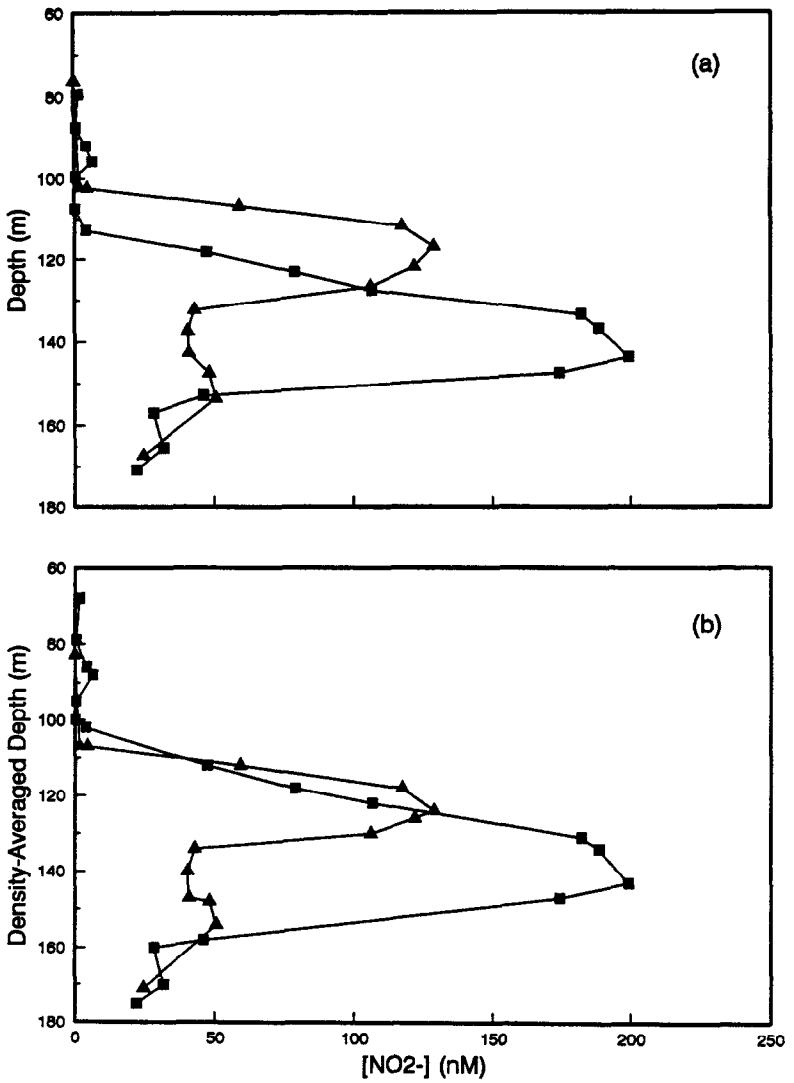


Fig. 5. Upper water column profiles of nitrite sampled 12 h apart during HOT-19 (July 1990). Horizontal axis is nitrite concentration in nM. Solid squares are from a cast begun at 04:00 h local time, solid triangles are from a cast begun that evening at 16:00 h. (a) Vertical axis shows *in situ* depth in m, emphasizing vertical displacement of features. (b) Vertical axis shows depth in m after employing density-averaging (as explained in the text), emphasizing concentration changes within features.

plotted against this density-averaged depth, the correspondence in the positioning of features in the nitrite profiles is evident. The remaining disparities between the two profiles must be due to *in situ* sources and sinks of nitrite. In this particular case, what is observed is a decrease in integrated nitrite (0–200 m) of 1.2 mmol m^{-2} in 12 h, which corresponds to a turnover time of about 2.6 days. We do not always see such rapid changes between profiles on a single cruise; however, since nitrification, phytoplankton nitrate reduction and phytoplankton nitrite assimilation are all strongly affected by light, and since internal

waves can move organisms and substrates at a particular isopycnal vertically 10s of meters through the light field in a few hours, it is not surprising that these short-term variations do occur. Similarly rapid changes in nitrite at the isopycnal associated with the PNM of 7.5–30 nmol l^{-1} h^{-1} also have been observed in the Southern California Bight (Ward, 1992).

Next let us examine nitrite variability on seasonal and longer timescales. A contour plot of nitrite concentration covering the upper 200 m from HOT-10 (September 1989) to HOT-50 (November 1993) is shown in Fig. 6. To filter the short-term depth fluctuations of isopycnals caused by internal wave motions we again use density-averaged depth, rather than the actual *in situ* depth at the time of the bottle trip. This filtering allows us to use multiple profiles from a single cruise (when available) and to examine longer-term trends without undoing short-term aliasing. Because the UPNM is an extremely sharp feature, the smoothing introduced by contouring yields a slightly lower maximum nitrite concentration than actually measured in an individual profile; nevertheless, a number of important trends in the smoothed data are evident.

We observe a distinct seasonality in the 5 and 25 nM contours, which can be used as an indicator of vertical mixing of nitracline waters into the surface layer. Upward excursions of these contours can be seen each year and are associated with winter water column instability; in a particularly strong event during HOT-14 (February 1990), the 5 nM contour nearly reached the sea surface. These observations are consistent with the hypothesized seasonality of mixing in the North Pacific gyre presented by Venrick (1993). The deepening

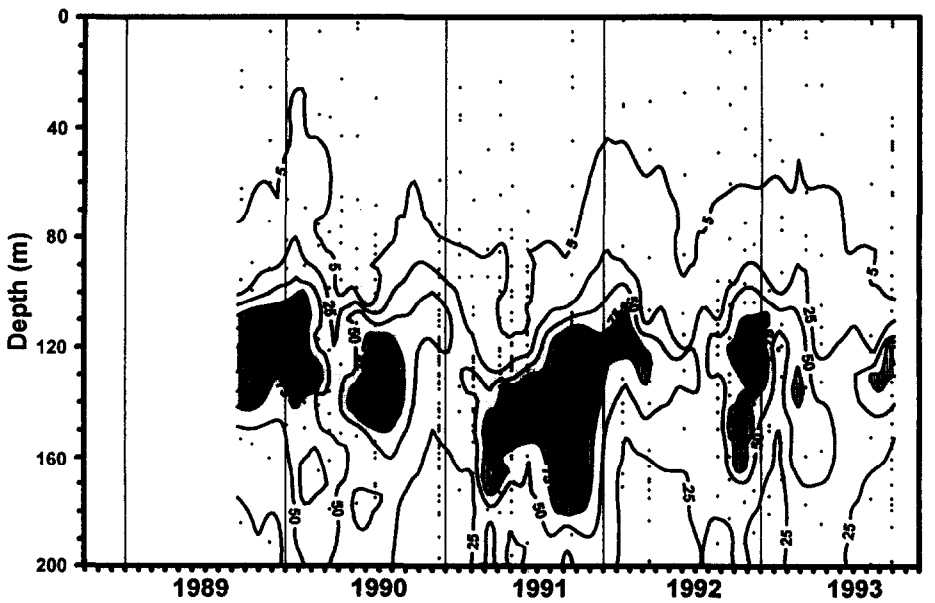


Fig. 6. Time-series contour plot of nitrite concentration in the upper 200 m at Station ALOHA during the first 5 years of the HOT program. Nitrite analyses were not begun until HOT-10 (September 1989). The horizontal axis represents time in calendar years, the vertical axis shows density-averaged depth in m (see text). Contours show [NO_2^-] in nM. Contour lines are located at 5, 25 and every 25 nM thereafter. Hatching is included where values exceed 75 nM and solid shading indicates values > 125 nM. Solid diamonds indicate where samples were collected.

of these contours in summer and early fall appears to be associated with the seasonal increase in light penetration. An abrupt deepening of the 25 nM contour is seen to some degree in the spring or early summer of each year and is pronounced in 1990. This feature does not seem to be associated with wind-driven mixing from the surface downward, but instead with some sort of density instability in the thermocline. The physical mechanism causing the isopycnals to deepen is not entirely clear, but appears to be a regular spring-time phenomenon.

Finally let us look at the positions of the UPNM and LPNM. We see three distinct times of year when the UPNM is intensified. Each winter, a shallow maximum develops, associated with vertical mixing; it is well-defined in 1989–1990 and 1992–1993, and discernable in 1990–1991 and 1991–1992. In spring, the UPNM deepens with the instability in the thermocline, clearly so in 1991 and 1993, less obviously in 1990 and 1992. Each summer/fall, slightly lagging the June maxima in light intensity, a robust UPNM develops. This feature is distinct in three of the years shown, but is not evident in 1992. Seasonality in the LPNM is not noted in this data set. In fact, because the LPNM is usually only a few nM in magnitude, its existence is masked by the large contour intervals used in Fig. 6. Only during HOT-19 (summer 1990) and HOT-31 (autumn 1991) does a distinct LPNM appear in the plot below the UPNM, yet within individual profiles a LPNM is often discernable (as in Fig. 4).

PNM structure and the nitracline

The nitrite profiles in the upper 200 m at Station ALOHA show the traditional features: a depleted surface layer with nanomolar–subnanomolar concentrations, a primary nitrite maximum, and a decrease into deeper waters. When examined in more detail, however, they reveal that the PNM is actually segregated into two layers: a large narrow UPNM that begins abruptly with the onset of the nitracline, and a low, broad LPNM, which rises above the depth-decaying nitrite tail. We suspect that the UPNM is maintained by the incomplete reduction of nitrate during assimilation by phytoplankton, and that the LPNM is the result of differential photoinhibition of the processes of ammonium oxidation and nitrite oxidation by nitrifying bacteria.

Herbland and Voituriez (1979) have compiled statistics on the relative vertical positions of the nitracline (which they defined as the first non-zero nitrate value as determined by standard colorimetric methods) and of the PNM at 123 stations across the tropical and subtropical Atlantic. They found a tight relationship, the PNM being on average about 11 m below the top of the nitracline. We use a slightly different procedural definition of the nitracline: we find the first sample that has $[NO_2^- + NO_3^-] > 100$ nM, then take the midway depth between it and the previous sample above, and relate the isopycnal at that depth to the average depth that the isopycnal was at during the cruise. This density-averaging filters out much of the effect of internal waves, allowing correlation of PNM depth and nitracline depth when the two constituents were not sampled from the same cast. Our data and a model II reduced major axis linear regression thereof are shown along with the Herbland and Voituriez (1979) regression (Fig. 7). Those authors used data from many different areas, with nitracline depths varying from about 15 to 105 m. Our data are from a single location over several years, thus cover less range in nitracline depths. Nevertheless, we see from Fig. 7 that over long times, large areas and different ocean basins, the strong correlation between the onset of the nitracline and the appearance immediately below the

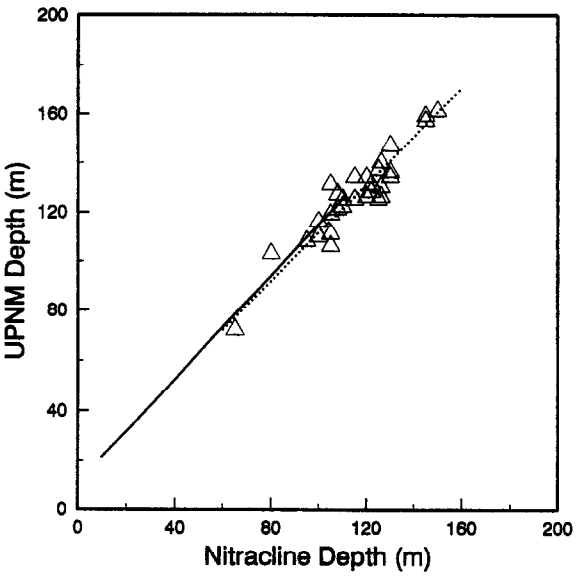


Fig. 7. Relationship between the positions of the upper primary nitrite maximum (UPNM) and the nitracline at Sta. ALOHA. The horizontal axis displays the depth associated with the nitracline, the vertical axis shows the depth associated with the UPNM. Both depths are density-averaged (see text) and expresed in m. Where the density-averaged depth of a feature differs between casts on a single cruise, the mean value is used. Open triangles are the actual data points from the 31 HOT cruises from which nitrite profiles were obtained. The dotted line is a reduced major axis model II linear regression of the data. The relationship determined by Herbland and Voituriez (1979) using data from 123 stations in the Atlantic is shown as a solid line.

UPNM is never compromised. Such a relationship is consistent with the direct measurements of nitrate assimilation rate made by Eppley and Koeve (1990), whose data show a distinct maximum in this rate about 10–15 m below the top of the nitracline.

Consider now the position of the nitrite maximum predicted by the nitrification model of Olson (1981a). For waters with such clarity as at Station ALOHA ($k_{par} \approx 0.036$–$0.044\ m^{-1}$) the Olson model predicts a low broad peak centered at about 130–140 m. Because internal wave motions frequently move isopycnals at Station ALOHA vertically 20 m or more in a single day, the average light level at a given isopycnal is higher than that measured at its average reference depth. The layer in which differential nitrification occurs is thus expected to be deeper than that predicted by the static model. We believe that the addition of 10 m to the depth of the Olson PNM is reasonable and conservative. Thus the Olson PNM should be located at about 140–150 m, which is not consistent with the shallow depth of the UPNM. Nor is the low, broad shape of the Olson peak consistent with the strong, steep UPNM that we observe. A time-series of UPNM position and nitracline position shows their coherence and offset (Fig. 8). The average ($\pm$sd) depths of the UPNM and nitracline are found to be 126 ± 18 m and 115 ± 18 m, respectively. Also shown is the position of the LPNM on 11 occasions when it was distinctly present. Its average depth is 149 ± 15 m, which is much more consistent with the feature predicted by the modified Olson model. Furthermore, the UPNM tracks the nitracline even when the latter is as shallow as 65 m (as in February 1993; Fig. 8), a depth at which light levels should be sufficient to inhibit nitrification completely.

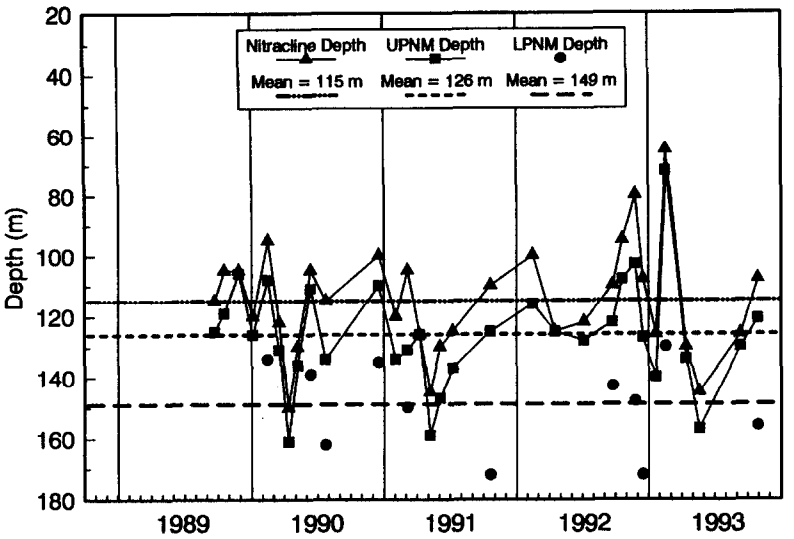


Fig. 8. Time-series of the positions of the nitracline, upper primary nitrite maximum (UPNM) and lower primary nitrite maximum (LPNM) at Sta. ALOHA. Horizontal axis gives time as calendar years, vertical axis displays density-averaged depth (see text) in m. Solid triangles represent the position of the nitracline, solid squares the UPNM and solid circles the LPNM. Mean associated depths over the displayed time period are indicated by broken lines as shown.

The PNM and particle flux

Both nitrite-forming processes within the PNM, the excretion of nitrite by phytoplankton and the oxidation of ammonium to nitrite by nitrifying bacteria, can be associated with the gravitational export of particulate organic matter. Phytoplankton nitrite excretion is a result of nitrate assimilation in the lower euphotic zone, representing new production that is available for export. Nitrification is fueled by the ammonium regenerated from organic nitrogen, which may in turn have particle-associated nitrogen as a source. We therefore hypothesized that the integrated 0–200 m nitrite and the sinking particulate nitrogen collected in our 150 m sediment traps may co-vary in time.

During the period from HOT-10 (September 1989) through to HOT-28 (July 1991), the integrated nitrite and the particulate nitrogen flux are fairly well correlated, as expected (Fig. 9). The peaks and valleys in the time-series of nitrogen flux are either contemporaneous with or lag slightly the corresponding features in the nitrite record. However, from HOT-28 (July 1991) to HOT-50 (November 1993) the relationship breaks down. Nitrite still shows considerable temporal variability, while particle flux decreases in both magnitude and variability and ceases to vary with nitrite.

The mechanism responsible for the observed changes in the characteristics of the particle flux is not entirely clear, but this and other equally dramatic changes in ecosystem parameters at Station ALOHA have been noted over the same time period, and may be related to the 1991–1992 ENSO event (Karl *et al.*, 1995, 1996). It is clear, though, that the integrated nitrite cannot be used under all conditions as an indicator of nitrogen export as we had originally hypothesized.

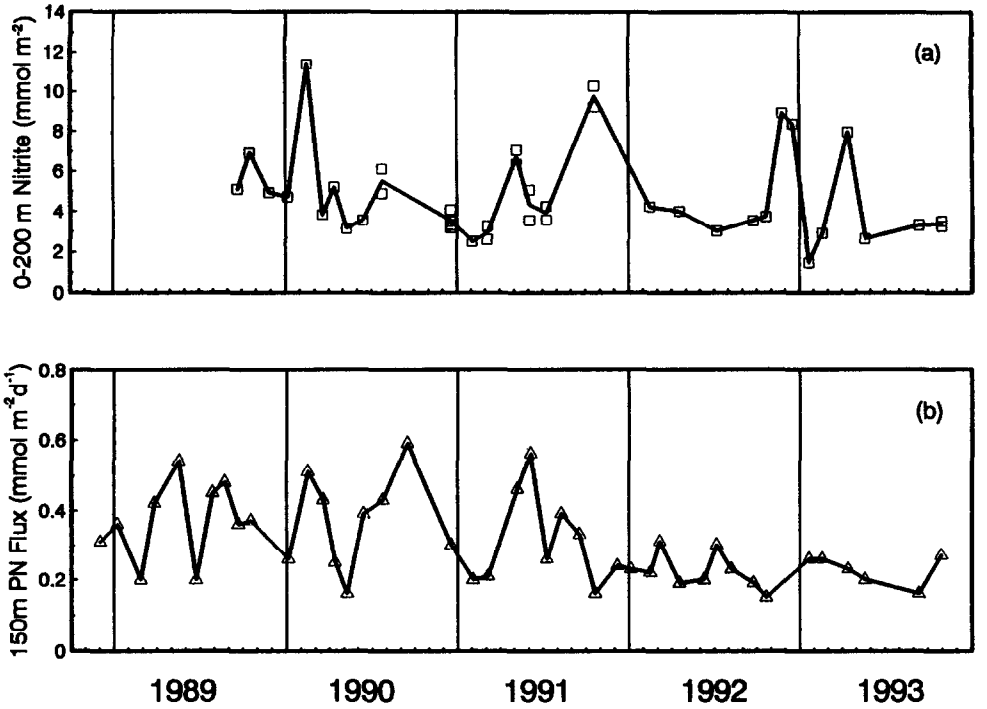


Fig. 9. Time-series of (a) 0–200 m depth-integrated nitrite and (b) mean particulate nitrogen flux at 150 m as collected by sediment traps at Sta. ALOHA. Integrated nitrite is expressed in mmol m^{-2} along the vertical axis, nitrogen flux in mmol m^{-2} day^{-1}. Horizontal axis displays time in calendar years.

Midwater and deep nitrite profiles

Nitrite distributions from seven HOT cruises measured over the 200–1000 m range show a supra-exponential decay from levels > 5 nM to levels < 1 nM over this depth interval (Fig. 10). An exception to this is the two-point maximum observed around 815–825 m during HOT-25 (April 1991). This part of the water column is within the oxygen minimum zone (Bingham and Lukas, 1996), and the elevated nitrite may be an expression of nitrification and/or denitrification processes occurring at low oxygen tension. It is not clear why this feature appears during only one of the seven cruises examined. Also shown in Fig. 10 is part of a published profile from the NW Atlantic (Columbus Iselin 8816, Sta. No. 1; Zafiriou *et al.*, 1992). Within the 200–1000 m range we find similar nitrite distributions to those measured in the Atlantic, both in shape and absolute magnitude. We also see concentration changes of a factor of two or more between cruises, indicating substantial variability on monthly timescales. These observations tend to support the hypothesis of rapid nitrite turnover in this part of the water column proposed by Zafiriou *et al.* (1992).

Our measured nitrite concentrations from 1000 m to within a few meters of the bottom at 4800 m, collected during the same seven cruises as above, are presented in Fig. 11. Concentrations of nitrite in these waters are low, and, with the exception of the near-bottom sample from HOT-25, all of these samples are ≤2 nM. Our values are substantially lower than those shown in the section presented by Wada and Hattori (1972), who reported

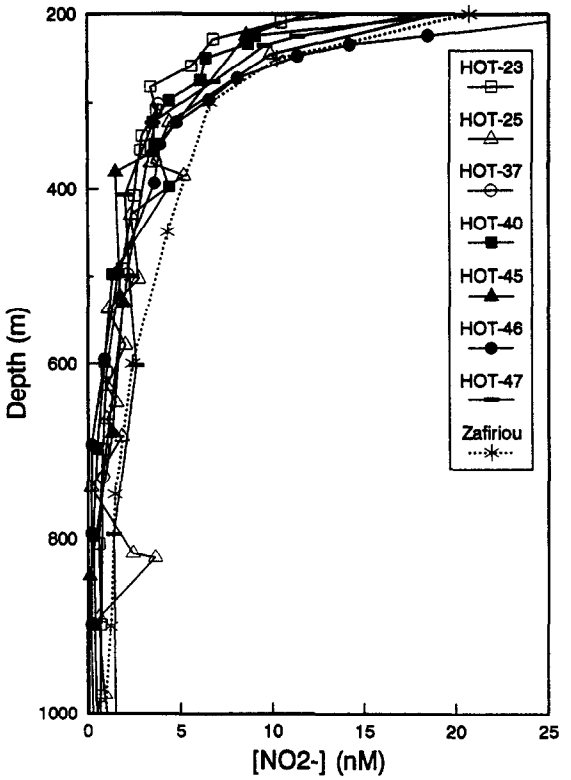


Fig. 10. Midwater profiles of nitrite from Station ALOHA. Horizontal axis is nitrite concentration in nM, vertical axis is depth in m. Individual cruises are as labeled. The asterisks and dotted line show for comparison data from the NW Atlantic published by Zafiriou *et al.* (1992).

concentrations up to 12 nM in waters deeper than 1000 m yet well above the seafloor. As their section passed within about 300 km of our study site, we must conclude either that horizontal or temporal nitrite variability in the deep ocean is large enough to account for these differences or that the analytical method used by these investigators suffered from difficulties at the low end of the concentration range. Because our values are much more consistent with those from the Atlantic, which Zafiriou *et al.* (1992) obtained using methods similar to ours, we suspect the latter is at least partly responsible for the discrepancy.

Four of our seven deep nitrite profiles show enrichments in the 4500–4800 m range with respect to their concentrations in the 3800–4300 m range above. In the HOT-25 profile this near-bottom enrichment is especially pronounced. Such enrichments also have been documented in the tropical Atlantic and Caribbean by Zafiriou *et al.* (1992). Rather than being anomalous, they may be a common feature of the deep ocean sediment–water interface. Because these bottom effects extend up 300 m or more from the ocean floor, and because they vary in magnitude, they may be indicators of variability in the intensity of sedimentary or nepheloid layer nitrogen cycle processes.

In deep waters, above the potential influence of the sediments, the rates of nitrogen cycle processes are expected to be very slow. However, we see up to 2 nM changes in deep nitrite on monthly-to-yearly timescales (Fig. 11). While this concentration change is small, when

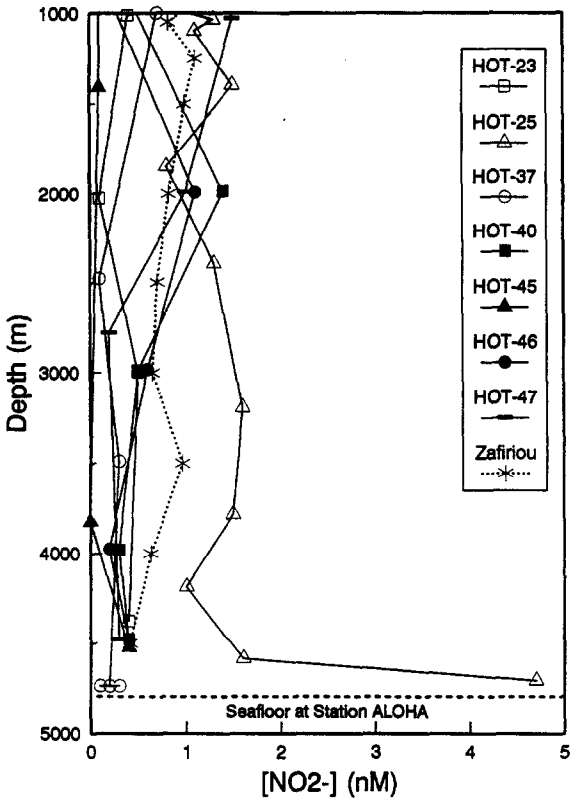


Fig. 11. Deep water profiles of nitrite from Station ALOHA. Horizontal axis is nitrite concentration in nM (but different in scale from Fig. 10), vertical axis is depth in m. Individual cruises are as labeled. The asterisks and dotted line show for comparison data from the NW Atlantic published by Zafiriou *et al.* (1992).

integrated over a 4000 m layer it represents a total nitrite change of 8 mmol m^{-2}, more than is usually found within the entire euphotic zone. This indicates that substantial month-to-month variability in the rates of deep nitrogen cycle processes and/or in the rate of supply of nitrogenous substrates exists in the deep Pacific.

It is unlikely that this large change in the deep nitrite pool results from nitrification, since the ammonium substrate would have to be derived from a substantial fraction of the annual gravitational export of particulate nitrogen (see Fig. 9(b)). We suspect that the increase in deep nitrite is derived from the large (*ca* 40 μM) pool of nitrate. This can be accomplished by free-living nitrate-reducing bacteria (Wada and Hattori, 1972), or by the living phytoplankton cells and/or associated bacteria found in pulses of phytodetritus reaching the seafloor at Station ALOHA. Such "fresh" phytodetritus has been collected in bottom-moored sediment traps at Station ALOHA (unpublished HOT data), and it is possible that the sinking cells have enough stored energy reserves to make a fruitless attempt at nitrate assimilation on their way to the seafloor. This would explain both the change in nitrite throughout the aphotic zone and the elevated nitrite concentrations near the bottom where the cells accumulate. While we do not have concurrent bottom-moored trap data and deep

nitrite data, we did observe a substantial particulate nitrogen flux with our free-floating traps during HOT-25 (Fig. 9(b)), contemporaneous with the elevated deep nitrite concentration measurements and consistent with this nitrate reduction hypothesis.

CONCLUSIONS

We have measured the distribution of nitrite and its variability at Station ALOHA over a 4 year period using chemiluminescent measurement techniques. In the upper 200 m of the water column, we consistently find a depleted surface layer, a primary nitrite maximum (PNM) and a supra-exponential decay into deeper waters. Upon closer inspection, we find that the PNM is actually a two-peaked structure: it is comprised of a large upper maximum (UPNM) associated at all times with the nitracline, and a lower peak (LPNM) that is not always discernable but at times may rival the UPNM in magnitude. We believe that the former is maintained by the reduction of nitrate during its assimilation by phytoplankton, and that the latter is maintained by differential nitrification. We also find that, despite initially favorable results, the nitrite content of the upper 200 m is not a consistent indicator of particulate nitrogen export.

Below 200 m, the concentration of nitrite continues to decay to nanomolar and often sub-nanomolar levels. The magnitude and curvature of the distribution below 200 m closely resemble those measured in the Atlantic, arguing against significant basin-to-basin differences in the deep nitrite pool. As in the Atlantic, near-bottom nitrite enrichments are noted sometimes at Station ALOHA. Substantial temporal nitrite variability exists on monthly-to-yearly timescales in the 200–4800 m layer, indicating dynamic nitrogen cycling even at great depths. Nitrate reduction by sinking phytoplankton cells may be responsible for observed increases in the deep nitrite pool.

Acknowledgements—The authors gratefully acknowledge all the members of the Hawaii Ocean Time-series project for their dedication and assistance with this work. Special thanks go to D. Hebel and R. Letelier for their frequent help with sampling and logistics. We also thank the captains and crews of the Research Vessels *Alpha Helix*, *Kaimalino*, *Kila*, *Moana Wave*, *New Horizon*, *Thomas G. Thompson*, *Townsend Cromwell* and *Wecoma* for their talented support of this project. This work was supported by National Science Foundation grants OCE87-17195 (R. Lukas, P.I.), OCE88-00329 (D. Karl, P.I.) and OCE93-01368 (D. Karl, P.I.), and by a fellowship from the Research Corporation of the University of Hawaii awarded to J. E. Dore. SOEST contribution no. 4062 and U.S. JGOFS contribution no. 224.

REFERENCES

Ambe M. (1978) Note of the experience in the preparation of CSK standard solutions and the ICES–SCOR intercalibration experiment, 1969–1970. *Marine Chemistry*, **6**, 171–178.

Bingham F. and R. Lukas. (1996) Seasonal cycles of temperature, salinity and dissolved oxygen observed in the Hawaii Ocean Time-series. *Deep-Sea Research II*, **43**, 199–213.

Brandhorst W. (1959) Nitrification and denitrification in the eastern tropical North Pacific. *Journal du Conseil Permenent International pour l'Exploration de la Mer*, **25**, 2–20.

Brzezinski M. A. (1988) Vertical distribution of ammonium in stratified oligotrophic waters. *Limnology and Oceanography*, **33**, 1176–1182.

Codispoti L. A. and F. A. Richards (1976) An analysis of the horizontal regime of denitrification in the eastern tropical North Pacific. *Limnology and Oceanography*, **21**, 379–388.

Cox R. D. (1980) Determination of nitrate and nitrite at the parts per billion level by chemiluminescence. *Analytical Chemistry*, **52**, 332–335.

Dore J. E., T. Houlihan, D. V. Hebel, G. Tien, L. Tupas and D. M. Karl. (submitted) Freezing as a method of sample preservation for the analysis of dissolved inorganic nutrients in seawater. *Marine Chemistry*.

Eppley R. W. and W. Koeve (1990) Nitrate use by plankton in the eastern subtropical North Atlantic, March–April 1989. *Limnology and Oceanography*, **35**, 1781–1788.

Fiadeiro M. and J. D. H. Strickland (1968) Nitrate reduction and the occurrence of a deep nitrite maximum in the ocean off the west coast of South America. *Journal of Marine Research*, **26**, 187–201.

French D. P., M. J. Furnas and T. J. Smayda (1983) Diel changes in nitrite concentration in the chlorophyll maximum in the Gulf of Mexico. *Deep-Sea Research*, **30**, 707–722.

Garside C. (1982) A chemiluminescent technique for the determination of nanomolar concentrations of nitrate and nitrite in seawater. *Marine Chemistry*, **11**, 159–167.

Herbland A. and B. Voituriez (1979) Hydrological structure analysis for estimating the primary production in the tropical Atlantic Ocean. *Journal of Marine Research*, **37**, 87–101.

Karl D. M. and R. Lukas (1996) The Hawaii Ocean Time-series (HOT) program: Background, rationale and field implementation. *Deep-Sea Research II*, **43**, 129–156.

Karl D. M., G. A. Knauer, J. H. Martin and B. B. Ward. (1984) Bacterial chemolithotrophy in the ocean is associated with sinking particles. *Nature*, **309**, 54–56.

Karl D. M., R. Letelier, D. Hebel, L. Tupas, J. Dore, J. Christian and C. Winn (1995) Ecosystem changes in the North Pacific subtropical gyre attributed to the 1991–92 El Niño. *Nature*, **373**, 230–234.

Karl D. M., J. R. Christian, J. E. Dore, D. V. Hebel, R. M. Letelier, L. M. Tupas and C. D. Winn (1996) Seasonal and interannual variability in primary production and particle flux at Station ALOHA. *Deep-Sea Research II*, **43**, 539–568.

Kiefer D. A. and J. N. Kremer (1981) Origins of vertical patterns of phytoplankton and nutrients in the temperate, open ocean: A stratigraphic hypothesis. *Deep-Sea Research*, **28**, 1087–1105.

Kiefer D. A., R. J. Olson and O. Holm-Hansen (1976) Another look at the nitrite and chlorophyll maxima in the central North Pacific. *Deep-Sea Research*, **23**, 1199–1208.

Letelier R. M., J. E. Dore, C. D. Winn and D. M. Karl (1996) Seasonal and interannual variations in photosynthetic carbon assimilation at Station ALOHA. *Deep-Sea Research II*, **43**, 467–490.

Miyazaki T., E. Wada and A. Hattori (1973) Capacities of shallow waters of Sagami Bay for oxidation and reduction of inorganic nitrogen. *Deep-Sea Research*, **20**, 571–577.

Miyazaki T., E. Wada and A. Hattori (1975) Nitrite production from ammonia and nitrate in the euphotic layer of the western North Pacific Ocean. *Marine Science Comm.*, **1**, 381–394.

Olson R. J. (1981a) Differential photoinhibition of marine nitrifying bacteria: a possible mechanism for the formation of the primary nitrite maximum. *Journal of Marine Research*, **39**, 227–238.

Olson R. J. (1981b) ^{15}N tracer studies of the primary nitrite maximum. *Journal of Marine Research*, **39**, 203–226.

Rakestraw N. W. (1936) The occurrence and significance of nitrite in the sea. *Biology Bulletin (Woods Hole)*, **71**, 133–167.

Schulenberger E. (1978) The deep chlorophyll maximum and mesoscale environmental heterogeneity in the western half of the North Pacific central gyre. *Deep-Sea Research*, **25**, 1193–1208.

Strickland J. D. H. and T. R. Parsons (1972) *A practical handbook of seawater analysis.* Bulletin No. 167, 2nd edition, Ottawa: Fisheries Research Board of Canada.

Takenaka N., A. Ueda and Y. Maeda (1992) Acceleration of the rate of nitrite oxidation by freezing in aqueous solution. *Nature*, **358**, 736–738.

Vaccaro R. F. and J. H. Ryther (1960) Marine phytoplankton and the distribution of nitrite in the sea. *Journal du Conseil Permenent International pour l'Exploration de la Mer*, **25**, 260–271.

Venrick E. L. (1993) Phytoplankton seasonality in the central North Pacific: The endless summer reconsidered. *Limnology and Oceanography*, **38**, 1135–1149.

Wada E. and A. Hattori (1971) Spectrophotometric determination of traces of nitrite by concentration of azo dye on an ion-exchange resin, application to sea waters. *Analytica Chimica Acta*, **56**, 233–240.

Wada E. and A. Hattori (1972) Nitrite distribution and nitrate reduction in deep sea waters. *Deep-Sea Research*, **19**, 123–132.

Wada E. and A. Hattori (1991) *Nitrogen in the sea: Forms, abundances, and rate processes*, CRC Press, Boca Raton, FL, U.S.A., 208 pp.

Ward B. B. (1992) The subsurface methane maximum in the Southern California Bight. *Continental Shelf Research*, **12**, 735–752.

Ward B. B. and O. C. Zafiriou (1988) Nitrification and nitric oxide in the oxygen minimum of the eastern tropical North Pacific. *Deep-Sea Research*, **35**, 1127–1142.

Ward B. B., K. A. Kilpatrick, E. H. Renger and R. W. Eppley (1989) Biological nitrogen cycling in the nitracline. *Limnology and Oceanography*, **34**, 493–513.

Zafiriou O. C., L. A. Ball and Q. Hanley (1992) Trace nitrite in oxic waters. *Deep-Sea Research*, **39**, 1329–1347.